A QUICK SOL-GEL PROCESS TO ELABORATE A HIGH BIOACTIVE CERAMIC POWDER

Bui Xuan Vuong[1], Nguyen Ngọc Thy[2], Do Quang Minh[2]

[1]Ho Chi Minh City Industry and Trade College; vuongbx@yahoo.com

[2]Ho Chi Minh City University of Technology; ngocthy0101@yahoo.com; m_doquang@yahoo.com

Abstract - A bioactive ceramic powder containing 45% SiO_2, 24.5% CaO, 24.5% Na_2O and 6% P_2O_5 (wt%) has been synthesized by a quick sol-gel process. Resulting material was investigated by several physico-chemical methods. The X-ray diffraction showed the presence of two crystalline phases, $Na_6Ca_3Si_6O_{18}$ and $NaCaPO_4$, in the structure of ceramic powder. The specific surface area and porosity were determined using the Brunauer – Emmet – Teller (BET) technique based on N_2 gas absorption-desorption. ''In vitro'' experiments were carried out by soaking the powder samples in simulated body fluid (SBF) at different times. X-ray diffraction (XRD), Fourier Transformed Infrared Spectroscopy (FTIR) and Scanning Electron Microscopy (SEM) coupled with Energy Dispersive X-ray Spectroscopy (EDS) were used for the ''in vitro'' evaluation of the bioactivity. The obtained results confirmed that the ceramic powder can be used as biomaterial for bone tissue engineering due to its high bioactivity expressed by the rapid formation of a biological carbonated hydroxyapatite layer on its surface after ''in vitro'' assay.

Key words - bioactive glass; bioactivity; ceramic powder; heat treatment; hydroxyapatite.

1. Introduction

Bioactive glasses are traditionally elaborated by melting method. In this method; primary materials are melted at high temperature. The obtained liquid is quenched to form an amorphous material at room temperature. The first melt-derived bioglass 45S5 with composition 45% SiO_2 - 24.5% CaO - 24.5% Na_2O - 6% P_2O_5 (wt%) was elaborated by Larry Hench in 1969 [1-4]. Recently; the sol-gel method is widely used to elaborate bioglasses. This technique permits the reseacher to obtain a bioglass with high surface area in comparison with the melt-derived bioglass [5-7]. The high surface area of sol-gel bioglass enhances the interfacial reactions between the material and physiological environment. That accelerates the formation of biological apatite layer.

Many bioglasses have been formed by sol-gel method but the elaboration of a similar glass to the first one 45S5 has not yet been successfully because of its crystalline during sol-gel procedure [8]. Several studies reported the elaboration of quaternary SiO_2 – CaO - Na_2O – P_2O_5 bioglasses by sol-gel method but their compositions are very different from the 45S5 bioglass [9-11].

While the 45S5 bioglass elaborated by sol-gel process has not yet been obtained; a similar quaternary system with high bioactivity can be considered an alternative approach. In this study; we reported a quick sol-gel process to elaborate a ceramic powder having the same composition with bioglass 45S5. This ceramic powder revealed the high bioactivity after "in vitro" assay in SBF solution.

2. Experimental procedure

2.1. Materials

The sol-gel synthesis of ceramic powder needed the following materials: tetraethyl orthosilicate (TEOS) (Aldrich; 99%); triethyl phosphate (TEP) (Sigma-Aldrich; 99.8%); calcium nitrate tetrahydrate (Fluka Biochemika; 99%) and sodium nitrate (Sigma-Aldrich; 99%).

2.2. Elaboration of ceramic powder

The sol-gel elaboration of bioactive ceramic powder 45% SiO_2 - 24.5% CaO - 24.5% Na_2O - 6% P_2O_5 (wt%) includes the following steps. First; 6.242 g of TEOS and 0.616g of TEP were stirred in 15 ml of distilled water for 2 hours by magnetic agitation at 500 rpm. The pH value of mixture was adjusted to 1.5 using HNO_3 solution. Next; 4.127 g of $Ca(NO_3)_2.4H_2O$ and 2.688 g of $NaNO_3$ were respectively added in the mixture at 60-minute intervals. Then; 3 drops of 30% ammonia solution were poured. The mixture was continuously stirred for 4 hours to obtain a condensed gel. The resulting gel was frozen and then freeze-dried at -60°C for 24 hours to remove the residual water and ethanol. Finally; the dry gel was heated at 1000°C for 2 hours to be converted into ceramic powder. The synthesis protocols are summarized in Figure 1.

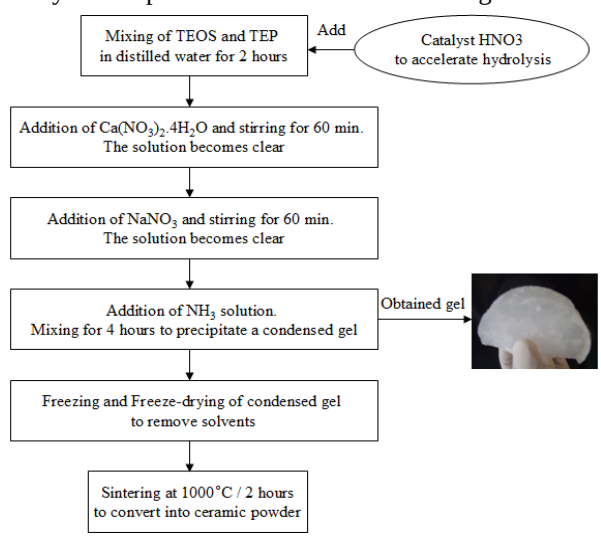

Figure 1. *Flowchart of the synthesis protocols of ceramic powder*

2.3. ''In vitro'' bioactivity test

Table 1. *Ionic concentrations (10^{-3} mol/l) of SBF solution and human blood plasma*

Ions	Na^+	K^+	Ca^{2+}	Mg^{2+}	Cl^-	HCO_3^-	HPO_4^{2-}
SBF	142	5	2.5	1.5	148.8	4.2	1
Plasma	142	5	2.5	1.5	103.0	27	1

''In vitro'' bioactivity of ceramic powder was investigated by soaking 100 mg of material in 200 ml of SBF solution at body temperature. The SBF composition is similar to that of human blood plasma as shown in Table 1.

It was prepared by dissolving NaCl; $NaHCO_3$; KCl; $K_2HPO_3.3H_2O$; $MgCl_2.6H_2O$ and $CaCl_2$ in distilled water and buffered with $(CH_2OH)_3CNH_2$ and HCl (6N) to adjust the pH value at 7.4 according to the Kokubo's method [12].

2.4. Physico-chemical characterizations

The ceramic powder before and after soaking in SBF solution were investigated by using several physico-chemical techniques. The specific surface and porosity of ceramic powder were determined by the N_2 adsorption-desorption measurements on multi point BET; ASAP 2010 Analyzer. In order to identify the crystalline phases of synthetic material and evaluate the formation of apatite layer after ''in vitro'' assay; X-ray diffraction (XRD) measurements were realized on Bruker D8 Advance diffractometer. Powder samples were mixed homogeneously with cyclohexane and dropped on the surfaces of plastic tablets. Then; these tablets were dried to remove the solvent and introduced into diffractometer. The XRD data was acquired in the range of 10-70° (2θ) with a scanning speed of 1°/min. The Fourier Transformed Infrared Spectroscopy (FTIR) (Bruker Equinox 55) was employed to identify the functional groups of the ceramic powder before and after ''in vitro'' assay. Powder materials were ground and mixed thoroughly with KBr powder in the ratio 1:100. FTIR spectra were recorded in the range of 400 and 4000 cm^{-1} wave number; at a resolution of 2 cm^{-1}. Scanning Electron Microscopy (SEM) (Jeol JSM 6301) coupled with Energy Dispersive X-ray Spectroscopy (EDS) was used to evaluate the morphological surface of ceramic powder as function of soaking time in SBF solution and determine the Ca/P elemental ratio in the apatite layer after ''in vitro'' assay.

3. Results and discussion

3.1. Physico-chemical characterizations of ceramic powder

3.1.1. Specific surface and porosity

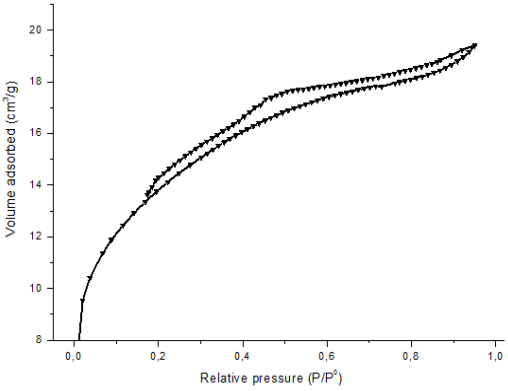

Figure 2. *N_2 absorption-desorption isotherm line of ceramic powder*

The N_2 absorption and desorption measurement was performed using multi-point BET. The graphical form of the BET isothermal line was presented in Figure 2. It exhibited a type IV isotherm according to the IUPAC classification; typical for a mesoporous material containing the pores between 2 and 50 nm in diameter. The data of the specific surface area; pore volume and pore size of ceramic powder were listed in Table 2. The surface area of the bioglass 45S5 was used for comparison [6]. The results showed that the specific surface area of ceramic powder was greatly higher than that obtained for the melt-derived glass 45S5.

Table 2. *Specific surface area and porosity of ceramic powder*

Samples	S_{BET} (m^2/g)	Pore volume (m^3/g)	Median pore diameter (nm)
Bioglass 45S5	0.15-2.7	-	-
Ceramic powder	47. 038	0.030	2.552

3.1.2. Identification of chemical composition by X-ray diffraction and IR spectroscopy

The XRD pattern of the sintered ceramic powder exhibited two crystalline phases as shown in Figure 3a. The identification of crystalline phases was performed using the database in the previous researches [12-13]. The major crystalline phase was determined $Na_6Ca_3Si_6O_{18}$. It was close to $Na_2Ca_2Si_3O_9$ phase which was found in heat treated 45S5 bioactive glass [14-15]. The minor phase was identified $NaCaPO_4$. Its existence illustrated the presence of phosphorus ions in the ceramic composition and was adapted to the chemical stoichiometry of the initial synthetic system.

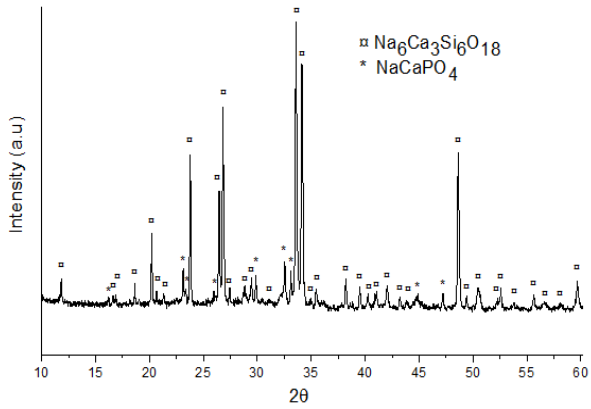

Figure 3a. *XRD diagram of ceramic powder*

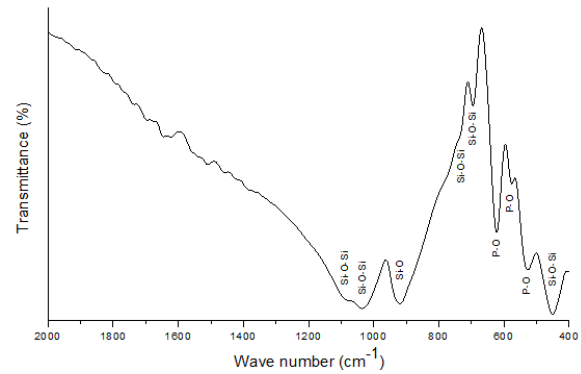

Figure 3b. *FTIR spectrum of ceramic powder*

The FTIR spectrum of ceramic powder presented the characteristic bands of a phospho-silicate network (Figure 3b). The identification of functional bands was referred to previous studies [15-17]. Three bands at 1094; 730 and 690 cm^{-1} were attributed to symmetric stretching Si-O-Si vibrations. The band at 1035 cm^{-1} was assigned to asymmetric stretching Si-O-Si vibration. The band at

920 cm^{-1} corresponded to Si-O bond. The band at 450 cm^{-1} attributed to an angular Si-O-Si deformation vibration. The presence of a sodium calcium phosphate crystalline was revealed by three characteristic bands at 620; 580 and 530 cm^{-1}. They were attributed to P-O bonds in $NaCaPO_4$ crystalline phase that was identified by X-ray diffraction.

3.2. Bioactivity of ceramic powder

3.2.1. X-ray diffraction and IR spectroscopy analysis

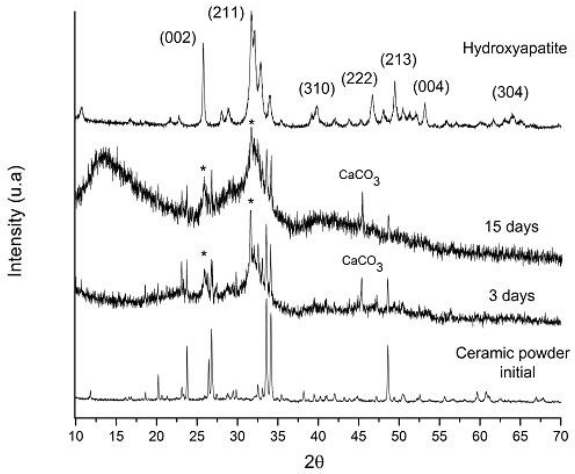

Figure 4. *XRD diagrams of ceramic powder before and after soaking in SBF solution*

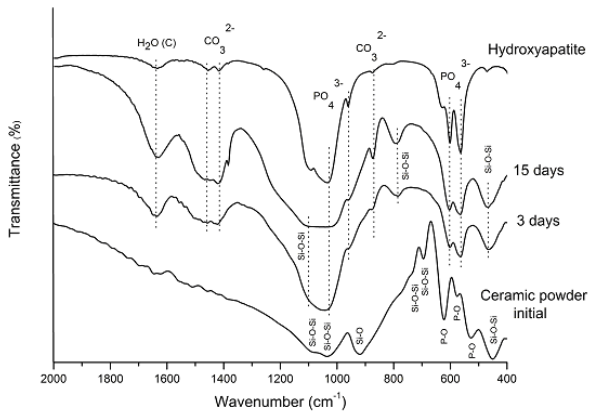

Figure 5. *FTIR spectra of ceramic powder before and after soaking in SBF solution*

Figure 4 showed the XRD diagrams of ceramic powder before and after soaking in SBF solution. The XRD diagram of hydroxyapatite was presented to evaluate the bioactivity of material as a function of immersion time [18]. After 3 days of soaking in SBF solution; the characteristic peaks of $Na_6Ca_3Si_6O_{18}$ phase became shorter or disappeared while two new peaks at 26° and 32° (2θ) emerged in the diffractogram of ceramic powder. These new peaks corresponded respectively to the (002) and (211) reflection planes in the structure of hydroxyapatite crystals. The obtained result confirmed the bioactivity of ceramic powder. The diffraction peaks of $Na_6Ca_3Si_6O_{18}$ phase continued to be short or disappeared while the intensities of two apatite characteristic peaks were not much modified from 3 days to 15 days. This result indicated that the apatite formation on the surface of ceramic powder could be completed almost after only 3 days of immersion.

Figure 5 showed the FTIR spectra of ceramic powder before and after soaking in SBF solution. The IR spectrum of synthetic hydroxyapatite was used as references to identify the formation of apatite phase on the surface of ceramic powder as function of soaking time [19]. After soaking in SBF solution; the initial structure of ceramic powder changed strongly due to the interfacial interactions between the material and the physiological solution. Consequently; the spectra of ceramic powder revealed new bands. In detail; the IR spectrum of ceramic powder emerged four new well-defined phosphate bands at 565; 603; 960 and 1039 cm^{-1} after 3 days of soaking in SBF solution. They were assigned to stretching vibrations of PO_4^{3-} groups in apatite crystalline phase. Two carbonate bands at 874 and 1420 cm^{-1} were also observed. The obtained results confirmed the formation of a carbonated hydroxyapatite layer on the surface of ceramic powder after ''in vitro'' assay. In addition; the IR spectrum of ceramic powder exhibited three new bands of Si-O-Si at 470 cm-1; 799 cm^{-1} (bending vibration) and 1070 cm^{-1} (stretching vibration) after soaking. They were characteristic of pure silica [4]. This result confirmed the formation of a SiO_2 gel on the surface of ceramic powder. That adapted to the interactive mechanism material-physiological solution described by Hench for a bioactive glass [1-3]. It was summarized following several steps such as: (1) Rapid exchange of protons H_3O^+ from the physiological solution with Ca^{2+}; Na^+ ions in bioglass to form the Si-OH groups; (2) Loss of soluble silica as $Si(OH)_4$ by breaking Si-O-Si bridging links and subsequent formation of silanol groups at the surface in this process; (3) Condensation and repolymerization of surface silanols to form SiO_2-rich surface layer; (4) Migration of Ca^{2+} and PO_4^{3-} from bioglass through the surface of the silica-rich layer and deposition of these ions from SBF solution to form an amorphous calcium phosphate (ACP) film on top of the SiO_2-rich layer; (5) Incorporation of OH^-; CO_3^{2-} from the solution and subsequent crystallization of the ACP layer to form a hydroxycarbonate apatite layer (HCA). After 15 days of soaking in SBF solution; the intensities of phosphate characteristic bands at 565; 603; 960 and 1039 cm^{-1} did not change much. This result is totally according to the XRD analyses; in which the characteristic peaks of hydroxyapatite did not change much from 3 to 15 days of immersion. The apatite layer could be formed totally on the surface of ceramic powder after 3 days of soaking in SBF solution. On the other hand; the characteristic bands of silica gel became more intensive after 15 days of immersion. This confirmed the growth of silica layer as function of soaking time in SBF liquid.

3.2.2. SEM and EDS analysis

Figure 6 showed SEM images of ceramic powder before and after soaking in SBF solution.

The initial morphological surface of ceramic powder was smooth. After immersion in SBF solution; it was modified strongly due to the interfacial chemical reactions between the ceramic powder and the physiological solution. After 1 day of immersion; the small particles began to form but the surface of ceramic powder was not much modified. After 3 days of

immersion; the surface of ceramic powder was covered completely with a homogeneous layer consisting of particles with identical form. This layer was attributed to the apatite layer formed on the surface of ceramic powder in according to the XRD and FTIR results; in which the ceramic powder significantly emerged the characteristic signs of apatite phase. The crystals of apatite grew with the soaking time in SBF solution. After 15 days of immersion; the surface of ceramic powder was covered with a dense and visible layer of apatite crystals. This result indicated that the crystalline quality of hydroxyapatite formed on the surface of ceramic powder increased with soaking time in SBF solution.

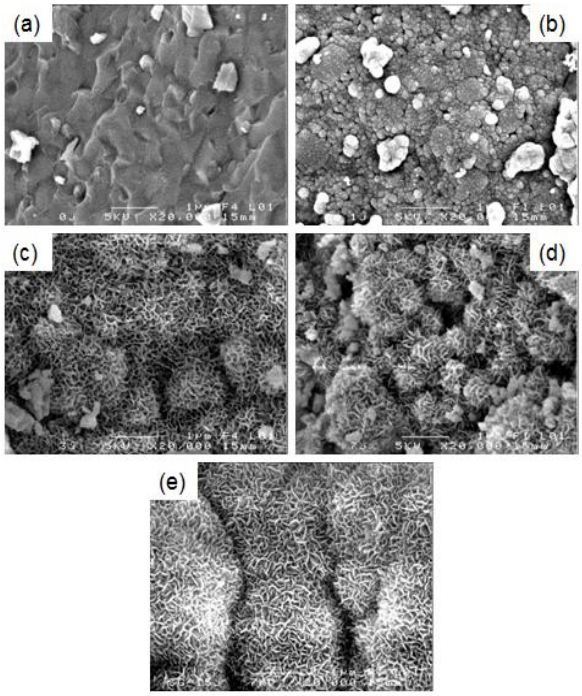

Figure 6. *SEM images of ceramic powder: (a) initial ceramic powder; (b) after 1 day; (c) after 3 days; (d) after 7 days and (e) after 15 days of soaking in SBF solution*

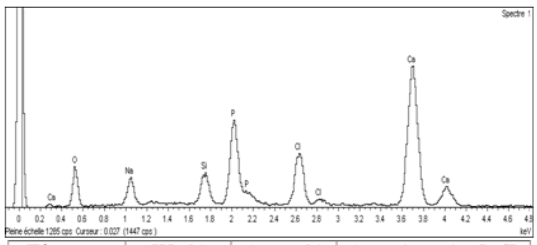

Element	Wt %	Atom %	Atomic ratio Ca/P
O	45.92	64.14	
Na	5.72	5.56	
Si	3.21	2.56	
P	11.95	8.62	13.86/8.62=1.61
Cl	8.34	5.26	
Ca	24.86	13.86	
Totality	100	100	

Figure 7. *EDS spectrum of ceramic powder after 15 days of soaking in SBF solution*

The EDS spectrum of ceramic powder after 15 days of immersion in SBF solution was shown in Figure 7. It showed the presence of Na; Si; P; Cl; Ca and O elements. The obtained phosphocalcium ratio Ca/P was of 1.61. It was nearly equal to the chemical stoichiometry of hydroxyapatite (Ca/P=1.67). This result explained the formation of bone like apatite on the surface of ceramic powder.

4. Conclusions

A bioactive ceramic powder containing 45% SiO_2 – 24.5% CaO - 24.5% Na_2O – 6% P_2O_5 (wt%) has been elaborated successfully using a quick sol-gel process. It consisted of two crystalline phases: $Na_6Ca_3Si_6O_{18}$ and $NaCaPO_4$. The "in vitro" assay was carried out by soaking ceramic samples in SBF solution at different times. The obtained results confirmed the bioactivity of this ceramic powder by the apatite formation within a few days.

REFERENCES

[1] L. L. Hench; R. J. Splinter; W. C. Allen WC; T. K. Greenlee; Bonding mechanisms at the interface of ceramic prosthetic materials*; J Biomed Mater Res 1971*; 5; 117-141.

[2] L. L. Hench; The story of bioglass; *J. Mater Sci: Mater Med 2006*;17; 967-978.

[3] L. L. Hench; J. K. West; Biological applications of bioactive glasses; *Life Chem Rep 1996*; 13; 187-241.

[4] E. Dietrich; H. Oudadesse; A. Lucas-Girot; M. Mami; "In vitro" bioactivity of melt-derived glass 46S6 doped with magnesium; *J Biomed Mater Res 2008;* 88A; 1087-196.

[5] R. Li; A. E. Clark; L. L. Hench; An investigation of bioactive glass powders by sol-gel processing; *J Appl Biomater 1991*; 2; 231-239.

[6] S. Sepulveda; J. R. Jones; L. L. Hench; Characterization of melt-derived 45S5 and sol-gel derived 58S bioactive glasses; *J Biomed Mater Res 2001;* 58; 734-740.

[7] L. L. Hench; A. E. Clark; R. Li; *Alkali-free bioactive sol-gel compositions;* United states patent 1991.

[8] A. Ramila; F. Balas; M. Vallet-Regi; Synthesis routes for bioactive sol–gel glasses: alkoxides versus nitrates*; J Chem Mater 2002*; 14; 542-558.

[9] M. Łączka; K. Cholewa-Kowalska; A. Łączka-Osyczka; M. Tworzydlo; B. Turyna; Gel-derived materials of a CaO-P_2O_5-SiO_2 system modified by boron; sodium; magnesium; aluminum; and fluorine compounds; *J Biomed Mater Res 2000*; 52; 601-612.

[10] D. Carta; D. M. Pickup; J. C. Knowles; M. E. Smithc; R. J. Newporta; Sol-gel synthesis of the P_2O_5-CaO-Na_2O-SiO_2 system as a novel bioresorbable glass; *J Mater Chem 2005*; 15; 2134-2140.

[11] X. Chatzistavrou; D. Esteve; H. Hatzistavrou; E. Kontonasaki; K. M. Paraskevopoulos; A. R. Boccaccini; Sol–gel based fabrication of novel glass-ceramics and composites for dental applications; *Mater Sci Eng C 2010*; 30; 730-739.

[12] T. Kokubo; H. Takadama; How useful is SBF in predicting in vivo bone bioactivity; *J Biomaterials 2006*; 27; 2907-3015.

[13] H. Ohsato; I. Maki; Y. Takeuchi; Structure of $Na_2CaSi_2O_6$; *Acta Crystallographica C 1985;* 41; 1575-1587.

[14] M. B. Amara; M. Vlasse; G. L. Flem; P. Hagenmuller; Structure of the low-temperature variety of calcium sodium orthophosphate; $NaCaPO_4$; *J Acta Crystallographica C 1983*; 39; 1483-1495.

[15] L. Lefebvre; L. Gremillard; J. Chevalier; R. Zenati; D. Bernache-Assolant; *Sintering behaviour of 45S5 bioactive glass*. *Acta Biomateriala 2008*; 4; 1894-1903.

[16] C. C. Lin; L. C. Huang; P. Shen; $Na_2CaSi_2O_6$-P_2O_5 based bioactive glasses. Part 1: Elasticity and structure; *J Non-Cryst Sol 2005*; 351; 3195-3203.

[17] L. Lefebvre; J. Chevalier; L. Gremillard; R. Zenati; G. Thollet; D. Bernache-Assolant; A. Govin; Structural transformations of bioactive glass 45S5 with thermal treatments; *J Acta Materiala 2007*; 55; 3305-3313.

[18] Fiche JCPDF 09-432.

[19] A. R. Boccaccini; Q. Chen; L. Lefebvre; L. Gremillard; J. Chevalier; Sintering; crystallisation and biodegradation behaviour of bioglass (R)-derived glass-ceramics; *Faraday Discuss 2007*; 136; 27-44.

(The Board of Editors received the paper on 08/30/2014; its review was completed on 05/25/2015)